Published as: *Neuron*. 2009 December 24; 64(6): 841–856.

Molecular Identification of Rapidly Adapting Mechanoreceptors and their Developmental Dependence on Ret Signaling

Wenqin Luo[1], **Hideki Enomoto**[2], **Frank L. Rice**[3], **Jeffrey Milbrandt**[4], and **David D. Ginty**[1,5]

[1]Solomon H. Snyder Department of Neuroscience, Howard Hughes Medical Institute, The Johns Hopkins University School of Medicine, Baltimore, MD, 21205-2185

[2]Laboratory for Neuronal Differentiation and Regeneration, RIKEN Center for Developmental Biology, Kobe, Japan

[3]Center for Neuropharmacology and Neuroscience, Albany Medical College, Albany, NY, 12208; Integrated Tissue Dynamics, LLC, Renssalaer, NY 12144

[4]Department of Pathology, Washington University School of Medicine, St. Louis, MO, 63110

Abstract

In mammals, the first step in the perception of form and texture is the activation of trigeminal or dorsal root ganglion (DRG) mechanosensory neurons, which are classified as either rapidly (RA) or slowly adapting (SA) according to their rates of adaptation to sustained stimuli. The molecular identities and mechanisms of development of RA and SA mechanoreceptors are largely unknown. We found that the "early Ret$^+$" DRG neurons are RA mechanoreceptors, which form Meissner corpuscles, Pacinian corpuscles and longitudinal lanceolate endings. The central projections of these RA mechanoreceptors innervate layers III through V of the spinal cord and terminate within discrete subdomains of the dorsal column nuclei. Moreover, mice lacking Ret signaling components are devoid of Pacinian corpuscles and exhibit a dramatic disruption of RA mechanoreceptor projections to both the spinal cord and medulla. Thus, the early Ret$^+$ neurons are RA mechanoreceptors and Ret signaling is required for the assembly of neural circuits underlying touch perception.

Introduction

The perception of form and texture is fundamental and essential for the daily lives of most, if not all animals. The first step in the perception of discriminative touch in mammals is the detection of pressure, vibration or stretch of the skin and deflection of hairs by specialized mechanosensory end-organs in the skin (Zelena, 1994). Low threshold, large-diameter trigeminal and dorsal root ganglion (DRG) neurons (mechanoreceptors) innervate these end-organs and are the primary sensory neurons mediating discriminative touch and tactile perception.

[5]To whom correspondence should be sent: dginty@jhmi.edu.

Additional materials and methods can be found in the Supplemental Data.

DRG mechanoreceptors can be classified according to the morphologies of their peripheral end organs, which include Merkel discs, Ruffini corpuscles, Meissner corpuscles, Pacinian corpuscles, and longitudinal lanceolate endings (Albrecht, 2008; Iggo and Andres, 1982). Glabrous skin contains Merkel discs and Meissner corpuscles, whereas general hairy skin contains Merkel discs and longitudinal lanceolate endings associated with guard hair follicles. Pacinian corpuscles are found in the dermis of humans, although in mice and rats they are normally restricted to joints and the periostium of bones (Zelena, 1994). Mechanoreceptors are further distinguished as being either rapidly adapting (RA) or slowly adapting (SA) based on their rates of adaptation to sustained mechanical stimuli (Mountcastle, 1957). Meissner corpuscles, Pacinian corpuscles and longitudinal lanceolate endings are RA mechanoreceptors (Iggo and Ogawa, 1977) whereas Merkel discs are the principle SA mechanoreceptors in rodents and monkeys (Iggo and Muir, 1969; Pare et al., 2002).

Despite physiological and morphological characterization of mechanoreceptor subtypes, mechanisms of development and unique functions of RA and SA mechanoreceptors are poorly understood, in part due to a lack of molecular identification of these neurons. Therefore, we have sought identification of candidate DRG mechanoreceptor subtypes based on a few broad criteria. First, since all mechanoreceptors are physiologically-defined “Aβ” fibers, then they are almost certainly large diameter, $NF200^+$ DRG neurons (Lawson et al., 1993). Also, mechanoreceptors, like proprioceptors, are born shortly after coalescence of rudimentary ganglia (Lawson et al., 1974). Furthermore, mechanoreceptors account for only a small percentage of all DRG neurons (Lawson et al., 1993). Therefore, candidate mechanoreceptors must be few in number, born shortly after DRG coalescence, and have large diameter soma sizes.

One approach to identify subtypes of DRG sensory neurons is to characterize them based upon their expression of receptors for neurotrophic factors. In fact, most if not all DRG neurons express receptors for one or more neurotrophic growth factors (Marmigere and Ernfors, 2007), which promote neuronal differentiation, maturation and survival. For example, small diameter, unmyelinated peptidergic nociceptors express the nerve growth factor (NGF) receptor TrkA, and are dependent upon NGF–TrkA signaling for expression of nociceptor-specific genes, innervation of the epidermis and survival (Crowley et al., 1994; Luo et al., 2007; Patel et al., 2000; Smeyne et al., 1994). Similarly, neurotrophins are involved in mechanoreceptor development and function. For example, the number of Merkel cells and their associated nerve terminals are decreased in P14 *NT3* mutant mice (Airaksinen et al., 1996), and BDNF is required postnatally for the normal transduction properties of SA mechanoreceptors (Carroll et al., 1998). In addition, overexpression of BDNF in the skin leads to enhanced innervation of hair follicles, large Meissner corpuscles, and an increase in the number of Merkel cells (LeMaster et al., 1999) while, conversely, Meissner corpuscles are absent in both *BDNF* and *TrkB* null mice (Gonzalez-Martinez et al., 2005; Gonzalez-Martinez et al., 2004; Perez-Pinera et al., 2008). However, Pacinian corpuscles and longitudinal lanceolate endings are present in normal numbers in all *neurotrophin* and *Trk* receptor mutant mice. Thus, the identity of trophic factors and their cognate receptors that support development of most populations of RA mechanoreceptors and their peripheral and central axonal projections is lacking.

The glia derived neurotrophic factor (GDNF) family of ligands (GFLs) contains four members, GDNF, neurturin (NRTN), artemin (ARTN) and persephin (PSPN) (Airaksinen and Saarma, 2002). The receptors for GFLs are comprised of a signaling subunit, the receptor tyrosine kinase Ret (Durbec et al., 1996; Trupp et al., 1996), and a GPI-anchored ligand binding subunit the GFL receptor (GFR) (Airaksinen et al., 1999). There are four GFRs in vertebrates, designated GFRα1 through GFRα4. *In vitro* binding assays indicate

that GDNF binds preferentially to GFRα1, NRTN to GFRα2, ARTN to GFRα3, and PSPN to GFRα4 (Airaksinen et al., 1999). *GFRα1*, *GFRα2*, *GFRα3*, but not functional *GFRα4* (Lindahl et al., 2000) are expressed in unique patterns in the DRG during development (Luo et al., 2007), suggesting key roles of GFL–GFR/Ret signaling in development of distinct populations of DRG sensory neurons.

Ret is expressed in approximately 60% of adult mouse DRG neurons, which can be broadly divided into two main groups based on their development history. Most Ret^+ DRG neurons are small to medium-diameter non-peptidergic nociceptors and are born around E11.5 or later and subsequently express *TrkA*. *Ret* is not highly expressed in these neurons until E15.5 or beyond (Luo et al., 2007; Molliver et al., 1997), and recent work has revealed a central role for Ret in their maturation and epidermal innervation (Luo et al., 2007). A distinct, smaller population consists of Ret^+ DRG neurons that are born earlier, express *Ret* prior to E11.5, do not express *TrkA* and have large soma diameters. These large diameter $Ret^+/TrkA^-$ neurons, which are referred to as the early Ret^+ neurons (Chen et al., 2006; Kramer et al., 2006; Luo et al., 2007; Marmigere and Ernfors, 2007; Molliver et al., 1997), caught our attention because they exhibit aforementioned features of mechanosensory neurons. Here, we show that the early Ret^+ DRG neurons are RA mechanoreceptors, which exhibit a modality-specific pattern of innervation of the brainstem and require Ret signaling for their assembly into neural circuits underlying discriminative touch perception.

Results

Molecular characterization of the early Ret^+ DRG neurons

We sought molecular identification and characterization of candidate mechanoreceptors which, like proprioceptors, are predicted to be early-born, large diameter, $NF200^+$ DRG neurons. One such neuronal population, the "early Ret^+" neurons, uniquely fits this profile. The early Ret^+ neurons are born during the first wave of DRG neurogenesis and begin to express *Ret* on or before E10.5, which is prior to initiation of expression of *TrkA* in the DRG (fig. S1A–C). Large diameter, $TrkC^+$ DRG neurons, some of which become proprioceptors (Klein et al., 1994), are born at approximately the same time. Interestingly, the early Ret^+ and $TrkC^+$ DRG neurons are distinct populations (fig. S1G–I, and (Kramer et al., 2006)). Moreover, while Ret is expressed exclusively in the early Ret^+ neurons ($Ret^+/TrkA^-$) in the DRG at E12 (Luo et al., 2007), it is expressed in many $TrkA^+$ DRG neurons ($Ret^+/TrkA^+$) beginning at E13.5 (fig. S1D–F). Furthermore, 54.3% ± 13.4% of early Ret^+ neurons co-express *TrkB* at E13.5 (fig. S1J–L), while only 25.1 ± 7.4% of the $TrkB^+$ DRG neurons co-express *Ret* (fig. S1J–L), indicating that *TrkB* is expressed in both early Ret^+ neurons as well as other DRG neurons at this time.

To characterize the early Ret^+ DRG neurons with respect to their expression of *GFRα* co-receptors, double fluorescent *in situ* hybridization experiments were performed using cRNA probes for *Ret* and *GFRαs* and sections from wild-type and *TrkA* null mice at different developmental stages. We found that *GFRα2* and *GFRα3* but not *GFRα1* are expressed in DRG neurons at E12 (Luo et al., 2007). At E13.5, *GFRα1–3* are expressed (Fig. 1A, D, G); *GFRα1* is co-expressed with *Ret* in many neurons (Ret^+ neurons: 17±4; $GFR\alpha1^+$ neurons: 17±5; and $GFR\alpha1^+/Ret^+$ neurons: 11±4 neurons/DRG section, Figure 1A–C) whereas all $GFR2^+$ neurons are Ret^+ (Ret^+ neurons: 18±2, $GFR\alpha2^+$ neurons: 9±2, and $GFR\alpha2^+/Ret^+$ neurons: 9±2. Figure 1D–F). In contrast, *GFRα3* is mainly expressed in Ret^- DRG neurons at this time (Ret^+ neurons: 21±6, $GFR\alpha3^+$ neurons: 51±9, and $GFR\alpha3^+/Ret^+$ neurons: 4±1. Fig. 1G–I). Therefore, we focused on *GFRα1* and *GFRα2* by analyzing their patterns of expression in *TrkA* null DRGs. *TrkA* null mice were used here because the expression of *Ret* and *GFRs* in late-born $Ret^+/TrkA^+$ DRG neurons is deficient in mice lacking TrkA signaling (Luo et al., 2007) while their expression in early $Ret^+/TrkA^-$ neurons should be

unaltered. At E13.5, approximately 80% of Ret$^+$ DRG neurons are lost in *TrkA* null DRGs (37 ± 6 vs. 7 ± 3 neurons/DRG, control vs. mutant, Fig. 1J–K), consistent with our finding that Ret$^+$/TrkA$^+$ DRG neurons are present in E13.5 wild-type (WT) DRGs. In addition, *GFRα2* exhibits a normal pattern of expression in *TrkA* mutant DRGs (Fig. 1 L–O); The number of GFRα2$^+$ DRG neurons in *TrkA* mutants is similar to that of WT controls (10 ± 3 vs. 9 ± 1, respectively), suggesting that at this time point, *GFRα2* is expressed exclusively in Ret$^+$/TrkA$^-$ neurons (the early Ret$^+$ DRG neurons). On the other hand, *GFRα1* is expressed exclusively in Ret$^+$/TrkA$^+$ DRG neurons at E13.5 since GFRα1$^+$ neurons are completely absent in DRGs of the *TrkA* mutant (29 ± 3 vs. 0, Fig. 1L–M). Similar results were obtained in experiments using P0 pups (fig. S2). Therefore, the early Ret$^+$ neurons express *GFRα2*, but not other *GFRαs*. A second, intermediate population of Ret$^+$ neurons emerges from TrkA$^+$ precursors, beginning ~E13.5, and expresses *GFRα1*. In addition, the non-peptidergic sensory neurons, which also originate from TrkA$^+$ precursors, express *Ret* beginning ~E16 and *GFRα2* from P0 onward (Luo et al., 2007). Thus, at least three distinct populations of Ret$^+$ DRG sensory neurons can be classified based upon their soma sizes, temporal patterns of *Ret* expression and co-expression of *GFRαs* (Fig. 1P).

Genetic labeling of the early Ret$^+$ DRG neurons

To test the idea that the early Ret$^+$ neurons are mechanoreceptors, a genetic labeling approach was developed to visualize their central and peripheral axonal projections. Here, we took advantage of the observation that the early Ret$^+$ neurons are the only DRG neurons that express *Ret* prior to E12.5 We generated a *Ret-CreERT2* (*Ret^{ERT2}*) knockin mouse line (fig. S3) in which the spatial and temporal patterns of expression of an inducible form of Cre recombinase (*CreERT2*) (Feil et al., 1997) recapitulate expression of *Ret*. These *Ret^{ERT2}* mice were crossed to neuron-specific reporter mice (*Tau$^{f(mGFP)}$*) (Hippenmeyer et al., 2005), in which myristoylated green fluorescent protein (mGFP) is expressed following Cre-mediated recombination, to generate *Ret^{ERT2}; Tau$^{f(mGFP)}$* mice. We predicted that administration of the ERT2 ligand 4-hydroxytamoxifen (4-HT) to *Ret^{ERT2}; Tau$^{f(mGFP)}$* reporter mice prior to E12.5 would lead to expression of GFP exclusively in early Ret$^+$ DRG neurons (Fig. 2A). In contrast, administration of 4-HT to *Ret^{ERT2}; Tau$^{f(mGFP)}$* mice at E15.5 or later (fig. S4A) is predicted to lead to GFP expression in both the early Ret$^+$ neurons and late-born Ret$^+$ DRG neurons, which emerge from TrkA$^+$ precursors. Using this strategy, administration of 4-HT from E10.5 to E12.5 resulted in 280 ± 25 GFP-labeled neurons in L5 DRGs at P14 (Fig. 2B), which represents ~5% of all L5 DRG neurons at this time (Liu et al., 2007). To address labeling specificity, we co-stained GFP$^+$ neurons with antibodies against TrkA and Ret at both E15.5 and P0. The Early Ret$^+$ neurons should be TrkA$^-$ and Ret$^+$ at both ages. At E15.5, 92.5% of GFP$^+$ neurons were TrkA$^-$ whereas 86% of them were Ret$^+$ (Fig. 2C–E). Similar findings were obtained with P0 pups (Fig. 2F–H). At P14, 100% of GFP$^+$ neurons were Ret$^+$ (Fig. 2M), suggesting that the few GFP$^+$/Ret$^-$ neurons observed at E15.5 and P0 are either lost postnatally or express Ret dynamically. In contrast, 73.7% of GFP-labeled neurons in *Ret^{ERT2}; Tau$^{f(mGFP)}$* mice that received 4-HT at later ages (E15.5–E17.5) are TrkA$^+$ at P0 (fig. S4), indicating that late 4-HT treatment indeed labels both the early Ret$^+$ neurons and late-born populations of Ret$^+$ neurons. We estimate that greater than 60% of early Ret$^+$ neurons are labeled following administration of 4-HT to *Ret^{ERT2}; Tau$^{f(mGFP)}$* mice from E10.5 to E12.5 by comparing the number of GFP$^+$/TrkA$^-$ neurons (5 ± 1 neurons/ DRG section Fig. 2F–G) to that of Ret$^+$/TrkA$^-$ neurons at P0 (8 ± 3 neurons/ DRG (Luo et al., 2007)).

To further characterize the population of Ret$^+$ neurons labeled by administration of 4-HT from E10.5 to E12.5, we measured their soma sizes and examined their patterns of expression of GFRα2, NF200, CGRP, Parvalbumin and TrkB and binding to the lectin IB4. As expected, the GFP-labeled early Ret$^+$ DRG neurons have large soma sizes (average area:

587±102 μm^2, fig. S5A), and 72.9% ± 11% of GFP^+ neurons are $TrkB^+$ at P0 (fig. S5B–D). In addition, at P14, 100% of the GFP^+ neurons are $GFR\alpha2^+$ and $NF200^+$ (Fig. 2J–K, M). On the other hand, almost none of the GFP^+ neurons were found to express CGRP nor did they bind to IB4 (Fig. 2L–M), which are markers for peptidergic (Hokfelt, 1991) and non-peptidergic nociceptors (Lawson, 1992), respectively. Furthermore, GFP^+ neurons do not express Parvalbumin (fig. S5E–G), which labels proprioceptors (Carr et al., 1989). Thus, 4-HT treatment of $Ret^{ERT2}; Tau^{f(mGFP)}$ mice prior to E12.5 specifically labels the early Ret^+ neurons, and these large diameter, GFP^+ DRG neurons exhibit molecular features of mechanosensory neurons.

The "Early Ret^+" neurons innervate RA mechanosensory end organs

Next, we examined the relationship between GFP^+ fibers and the different mechanosensory end organs at P14, an age when they exhibit mature morphologies (Zelena, 1994). We first examined the innervation of Merkel discs using a TRPV3 antibody, which specifically labels Merkel cells (fig. S6A–F). We found that GFP^+ fibers are not associated with Merkel cells in the footpad (Fig. 3A–C), touch domes of back hairy skin, guard hair follicles, or regular glabrous skin (fig. S6G–O). Thus, the early Ret^+ neurons do not innervate Merkel cells and, therefore, they are not SA mechanosensory neurons. Instead, GFP^+ fibers innervate Meissner corpuscles (Fig. 3D–F), which are located in dermal papillae of the footpad. In hairy skin, GFP^+ fibers form longitudinal lanceolate endings associated with guard hair follicles (Fig. 3G–I). Furthermore, GFP^+ fibers innervate Pacinian corpuscles, which in mice are found in abundance in the periosteum of the fibula (Zelena, 1976) (Fig. 3J–L). Taken together, these findings suggest that the early Ret^+ DRG neurons are RA mechanosensory neurons.

Early Ret^+ DRG neurons exhibit a modality-specific pattern of axonal projections to the brainstem

Mechanoreceptors send collateral branches that innervate the dorsal horn of the spinal cord (Brown, 1981) and others that ascend ipsilaterally within the dorsal column (DC) to the gracile and cuneate nuclei (dorsal column nuclei, DCN) of the medulla (Carpenter MB, 1983). As expected, GFP-labeled central axonal projections enter the spinal cord at a dorsal-medial position and innervate layers III through V of the dorsal horn (Fig. 4A–G). GFP^+ axons also project within the gracile and cuneate fasciculi of the DC (Fig. 4A, H) and are highly enriched in the gracile fasiculus at cervical levels (Fig. 4H). In addition, GFP^+ fibers innervate both the gracile and cuneate nuclei (Fig. 5A, D, G), and remarkably, the termination zones of these axons within the DCN exhibit a unique pattern of zonal segregation. The entire extent of the DCN is clearly visualized and demarcated by the pattern of $VGLUT1^+$ synapses (Fig. 5B, E, H and (Hughes et al., 2007)) as well as the axonal terminations of primary sensory neurons in $Advillin^{AP}$ mice (data not shown), in which all somatosensory neurons are labeled with human placental alkaline phosphatase (Hasegawa et al., 2007). Within the DCN, GFP^+ axons terminate extensively within most of the gracile nucleus (Fig. 5 and fig. S7) except for a small dorsal-rostral zone (Fig. 5D–F and fig. S7), which is rich in VGLUT1 synapses but lacks GFP^+ terminations. In the cuneate nucleus, by contrast, many GFP^+ fibers terminate within a medial-rostral zone (Fig. 5A–C and fig. S7) while the ventral-caudal region of the cuneate nucleus is virtually devoid of GFP^+ endings (Fig. 5D–I and fig. S7). These findings reveal specific termination zones of the early Ret^+ DRG neurons within the DCN of the mouse brainstem (Fig 5J), the pattern of which is remarkably similar to those of RA mechanoreceptors revealed by physiological recordings in cats (Dykes et al., 1982). Based on the peripheral and central patterns of GFP^+ axonal projections, we conclude that the early Ret^+ DRG neurons are RA mechanoreceptors.

Peripheral and central projections of early Ret+ DRG neurons in *Ret*$^{f(CFP)}$; *Wnt1*^{Cre} mice

To further characterize the pattern of innervation of mechanosensory end organs by Ret$^+$ DRG neurons, and to substantiate our findings using *Ret*^{ERT2}; *Tau*$^{f(mGFP)}$ reporter mice, described above, we made use of a Ret conditional CFP (*Ret*$^{f(CFP)}$) mouse line in which CFP is expressed in all Ret$^+$ cells following CRE-mediated recombination (Uesaka et al., 2008). For these experiments, *Ret*$^{f(CFP)}$ mice were crossed to a neural crest lineage mouse line, *Wnt1*^{Cre} mice (Danielian et al., 1998). Thus, in *Ret*$^{f(CFP)}$;*Wnt1*^{Cre} mice, CFP is expressed in all Ret$^+$ DRG neurons, including the early Ret$^+$ DRG neurons. Consistent with our findings described above, CFP$^+$ fibers do not innervate Merkel cells in glabrous skin or those associated with guard hair follicles in hairy skin (fig. S8A–C, and data not shown). Instead, CFP$^+$ fibers form Meissner corpuscles (fig. S8D–F), longitudinal lanceolate endings (fig. S8G–I), and Pacinian corpuscles (fig. S8J–L). Interestingly, although Wnt1^{Cre} is active in DRG neurons, Schwann cells and their precursors, only axons of DRG neurons are labeled with CFP (fig. S8F,L) indicating that *Ret* is expressed in RA mechanosensory DRG neurons but not Schwann cells or other neural crest-derived accessory cells. Furthermore, as expected, CFP$^+$ fibers innervate layers I through V in the spinal cord (fig. S8M–P) and are highly enriched in the gracile fasciculus at the cervical level of the spinal cord (data not shown). These peripheral and central patterns of GFP$^+$ axonal innervation indicate that a subpopulation of Ret$^+$ DRG neurons are RA mechanoreceptors, supporting the aforementioned analysis of the early Ret$^+$ DRG neurons using *Ret*^{ERT2}; *Tau*$^{f(mGFP)}$ reporter mice. Hereafter, we refer to the early Ret$^+$ DRG neurons as RA mechanoreceptors.

RA mechanosensory neurons lacking Ret signaling components are present in normal numbers in neonatal mice

The high levels of embryonic expression of Ret and GFRα2, the preferred co-receptor for NRTN (Jing et al., 1997), in RA mechanosensory neurons suggests a role for the NRTN–GFRα2/Ret signaling module in controlling development of these neurons. To test this idea, we first counted the number of RA mechanosensory neurons in *NRTN* null (Heuckeroth et al., 1999) and *GFRα2*^{GFP} knockin mice (McDonagh et al., 2007). We measured two parameters to evaluate the number of RA mechanoreceptors at P0: the number of Ret$^+$/TrkA$^-$ neurons in *NRTN* null mice and the number of large-diameter neurons expressing a high level of GFP in *GFRα2*^{GFP} knockin mice. In both cases, similar numbers of RA mechanosensory neurons were observed in wild-type and mutant animals (Ret$^+$/TrkA$^-$ neuron number in control and *NRTN* null mice: 10 ± 1 vs. 9 ± 1; GFP$^+$ neuron number in *GFRα2*^{GFP} heterozygous vs. homozygous mutant mice: 5± 1 vs. 4 ± 1) (fig. S8A–H). In addition, we counted TrkB$^+$ DRG neuron number in P0 control (21 ± 3/ DRG section), *Ret* (21 ± 3/ DRG section), *NRTN* (21 ± 5/DRG section) and *GFRα2* (20 ± 4/DRG section) null mice (fig. S10A–D), and found virtually identical numbers of TrkB$^+$ neurons in these mice, suggesting RA mechanoreceptors are present at P0 in the absence of Ret signaling. Consistent with these findings, our previous work revealed that normal numbers of large-diameter NF200$^+$ neurons are found at P14 in *Ret*$^{f/f}$;*Wnt1*^{Cre} mice (Luo et al., 2007). Taken together with the finding of normal numbers of cutaneous RA end organs in *Ret* mutants at P14, described below, we conclude that NRTN–GFRα2/Ret signaling is not required for survival of most if not all RA mechanosensory neurons, at least up to P14. Interestingly, though not required for survival, *Ret* and *NRTN* are required for maximal expression of *GFRα2* in RA mechanoreceptors as the level of *GFRα2* is diminished in both *Ret*$^{f/f}$;*Wnt1*^{Cre} and *NRTN* null DRGs at P0 (fig. S9A–C).

Since Ret signaling is not required for survival of RA mechanoreceptors and more than half of the early Ret$^+$ neurons express TrkB at E13.5 and P0 (fig. S1L and S5K), we next asked whether *TrkB* controls their survival. We found similar number of Ret$^+$/TrkA$^-$ DRG neurons in control and *TrkB*$^{f/f}$;*Wnt1*^{Cre} DRGs at P0 (6 ± 2 vs 5 ± 2, fig. S10E–J) indicating

that *TrkB,* like *Ret*, is not required for prenatal survival of most if not all RA mechanoreceptors.

A NRTN-GFRα2/Ret signaling cascade controls development but not maintenance of Pacinian corpuscles

Peripheral endings of RA mechanosensory neurons were next examined for their developmental dependence on Ret signaling. Meissner corpuscles and lanceolate endings are present in normal numbers in both $Ret^{f/f};Wnt1^{Cre}$ and *NRTN* mutants at P14 (Fig. 6C–D, G–H, fig. S11C, and data not shown) although many of these endings appear morphologically underdeveloped and disorganized (Fig. 6C–D, G–H, and fig. S11A–B). Since Meissner corpuscles and lanceolate endings constitute the majority of RA mechanoreceptors (Johansson and Vallbo, 1979), this result supports our conclusion that *Ret* is not required for survival of most RA mechanosensory neurons. On the other hand, mice lacking *TrkB* in all derivatives of the neural crest ($TrkB^{f/f};Wnt1^{Cre}$) (fig. S11D–I) or *TrkB* null mice (Fundin et al., 1997; Gonzalez-Martinez et al., 2005; Gonzalez-Martinez et al., 2004; Perez-Pinera et al., 2008) exhibit a complete absence of Meissner corpuscles and a modest morphological disorganization of lanceolate endings. Interestingly, $NF200^{+}$ fibers are present in the dermal papillae of the $TrkB^{f/f};Wnt1^{Cre}$ mice (fig. S11G–H), suggesting that mechansosensory axon terminals reach the dermal papillae but that morphological differentiation of the corpuscle fails in the absence of TrkB signaling.

In striking contrast, we found that the development of Pacinian corpuscles is absolutely dependent upon *Ret*. These mechanosensory end-organs are completely absent in the periostium of $Ret^{f/f};Wnt1^{Cre}$ mice (Fig. 6A–B, E–F and I–J; 35 ± 5 vs. 0 Pacinian corpuscles/periosteum membrane) as determined by both S100 immunostaining and H & E staining. Moreover, wholemount anti-S100 staining of the periosteum membrane reveals that the nerve branches that normally penetrate Pacinian corpuscles are absent in $Ret^{f/f};Wnt1^{Cre}$ mice (Fig. 6E–F). Since Ret is expressed in RA mechanosensory DRG neurons but not in the accessory cells of the corpuscle, (fig. S8L), Ret is required in RA mechanosensory neurons autonomously for Pacinian corpuscle formation. Remarkably, a similar phenotype is observed in both *NRTN* and $GFR\alpha2^{GFP}$ null mice (Fig. 6K–L), indicating that a NRTN–GFRα2/Ret signaling cascade controls development of Pacinian corpuscles. Consistent with previous findings (Gonzalez-Martinez et al., 2004; Perez-Pinera et al., 2008), $TrkB^{f/f};Wnt1^{Cre}$ mice exhibit normal numbers of Pacinian corpuscles (fig. S11 J and M).

While the NRTN–GFRα2/Ret signaling cascade is necessary for development of Pacinian corpuscles, it is not required for the maintenance of these mechanosensory end-organs once they have formed. 4-HT-mediated acute deletion of *Ret* in three week-old $Ret^{ERT2/f}$ mice (fig S12A–B) has no effect on the number or morphology of Pacinian corpuscles in mice as old as six months (Fig. S12C–D, G–H). This is in marked contrast to the dramatic loss of epidermal axonal endings of non-peptidergic nociceptors, observed in the same animals (fig. S12E–F, I–J). Thus, NRNT–GFRα2/Ret signaling is absolutely essential for development, but not maintenance of Pacinian corpuscles, while it cooperates with BDNF–TrkB signaling to control development and innervation of both Meissner corpuscles and longitudinal lanceolate endings.

Ret signaling controls central axonal projections of RA mechanosensory neurons

Since *Ret* is highly expressed in RA mechanosensory neurons when their axons extend into the spinal cord and then into the DCN within the medulla, we next addressed the possibility that Ret signaling controls this process. We first used VGLUT1 staining to visualize the synapses of central projections of all mechanoreceptors in $Ret^{f/f};Wnt1^{Cre}$ mice and their

littermate controls. Here, the intensity of VGLUT1 staining within layers III through V of the spinal cord was found to be markedly reduced in $Ret^{f/f};Wnt1^{Cre}$ mice (Fig. 7A, C, D). This deficit is specific for mechanosensory endings because the innervation of both Clarke's nucleus by proprioceptors (Fig. 7A, C, D) and layer II by non-peptidergic nociceptors (Luo et al., 2007) of the mutants is comparable to controls. In addition, the gracile nucleus is markedly smaller in $Ret^{f/f};Wnt1^{Cre}$ mice (Fig. 7B, E, F) compared to littermate controls. Furthermore, the VGLUT1 staining intensity within the gracile nucleus is dramatically reduced in $Ret^{f/f};Wnt1^{Cre}$ mice (Fig. 7B, E, G). In contrast, both the size and VGLUT1 staining intensity of the ventral-caudal region of the cuneate nucleus in $Ret^{f/f};Wnt1^{Cre}$ mice are similar to controls (Fig. 7B, E, F, G), which is consistent with our finding that RA mechanosensory terminations are restricted to the more medialrostral region of the cuneate nucleus. Interestingly, $TrkB^{f/f};Wnt1^{Cre}$ mice exhibit a normal pattern of VGLUT1 staining in both the spinal cord and medulla (fig. S11K, L, N,O). These results indicate that Ret, but not TrkB, is required for the formation of both branches of the central projections of RA mechanoreceptors.

Since VGLUT1 labels synapses of both RA and SA mechanoreceptors, it is possible that the central projection phenotypes observed in $Ret^{f/f};Wnt1^{Cre}$ mice reflect deficits of axonal projections of one or both of these mechanosensory populations. In addition, it is possible that *Ret* functions in a non-cell autonomous manner to affect RA mechanosensory projections to the spinal cord. Indeed, *Ret* is expressed in other populations of DRG neurons beginning at E13.5 as well as neurons in the dorsal spinal cord and medulla (Golden et al., 1999), all of which are subjected to Cre-mediated excision in $Ret^{f/f};Wnt1^{Cre}$ mice (data not shown). To distinguish between these possibilities and address the cell autonomy of *Ret* function, we sought to delete *Ret* in RA mechanosensory neurons but not other DRG or dorsal horn neurons. Here, we employed Ret^{ERT2} mice and the procedure of 4-HT treatment of mice prior to E12.5. Activation of Cre recombinase in spinal interneurons using this strategy is predicted to be minimal because expression of *Ret,* and hence Ret^{ERT2} is expressed in very few neurons in the dorsal spinal cord at E13.5 (data not shown). Indeed, we found that few spinal cord interneurons are labeled in $Ret^{ERT2};Tau^{mGFP}$ mice following three days of 4-HT treatment prior to E12.5 (Figure 4A, E). Therefore, we generated both $Ret^{ERT2};Tau^{f(mGFP)}$ control and $Ret^{ERT2/f(CFP)}$ conditional mutant mice, which enable selective visualization of the central projections of RA mechanosensory neurons that are either heterozygous or homozygous null for *Ret,* respectively. The $Ret^{ERT2/f(CFP)}$ mice harbor one Ret^{ERT2} allele, which is null, and one floxed *Ret* allele $f(CFP)$ which, following Cre-mediated excision is also null for *Ret* and expresses CFP (Uesaka et al., 2008). Thus, following 4-HT treatment at E11.5–E12.5, CFP^+ DRG neurons in $Ret^{ERT2/f(CFP)}$ mice are *Ret* null RA mechanosensory neurons while, in contrast, GFP^+ neurons in control $Ret^{ERT2};Tau^{f(mGFP)}$ mice are RA mechanosensory neurons harboring one functional *Ret* allele. We used two days instead of three days of 4-HT treatment for these experiments so that relatively few RA mechanosensory neurons would be labeled. The 4-HT-treated $Ret^{ERT2};Tau^{f(mGFP)}$ control mice serve as an excellent control for 4-HT-treated $Ret^{ERT2/f(CFP)}$ mutant mice because: 1) The level of expression of CFP in $Ret^{ERT2/f(CFP)}$ mutant DRG neurons is comparable to or higher than that of GFP in control $Ret^{ERT2};Tau^{f(mGFP)}$ neurons since CFP is directly visible in $Ret^{f(CFP)}$ mice following recombination while GFP in Tau^{mGFP} mice is not (data not shown); 2) Two days of 4-HT treatment of $Ret^{ERT2/f(CFP)}$ and control $Ret^{ERT2};Tau^{f(mGFP)}$ mice resulted in 6 ± 2 CFP^+ and 8 ± 3 GFP^+ neurons/DRG section at P14 (Fig. 7R,V), respectively, indicating the labeling efficiency in the two mouse lines is comparable, and; 3) Both GFP and CFP effectively localize to the central axons of mechanoreceptors innervating layers III through V of the spinal cord of control mice (Fig 2A, E, and fig. S8M). As predicted, 4-HT treatment at E11.5 –E12.5 of both control $Ret^{ERT2};Tau^{f(mGFP)}$ and mutant $Ret^{ERT2/f(CFP)}$ mice results in very few GFP^+ and CFP^+ spinal cord dorsal horn interneurons, respectively (Fig 7H, L), indicating that *Ret* is deleted

in very few spinal cord interneurons in *Ret*$^{ERT2/f(CFP)}$ mice. Therefore, any phenotype observed in RA mechanosensory neurons in *Ret*$^{ERT2/f(CFP)}$ mice reflects a cell autonomous function of *Ret* in these neurons. Using this strategy, we observed that while GFP^{+} neurons of *Ret*^{ERT2}; *Tau*$^{f(mGFP)}$ control mice robustly innervate lamina III through V of the spinal cord, CFP^{+}, *Ret* null neurons of *Ret*$^{ERT2/f(CFP)}$ mice exhibit a striking absence of axonal projections in both the spinal cord dorsal horn (Fig. 7H, L, K) and DC (Fig. 7I, J, M, N, O) of P14 mice. Moreover, there are fewer CFP^{+} projections in the gracile and cuneate nuclei of *Ret*$^{ERT2/f(CFP)}$ mutant mice (Fig. 7P,Q,T,U,S). Therefore, *Ret* is required cell autonomously for the extension of axonal branches of RA mechanosensory neurons into the spinal cord and the gracile and cuneate nuclei of the medulla.

To gain further insight into the nature of the central projection deficit of *Ret* null RA mechanoreceptors, we analyzed the axons of *Ret*$^{ERT2/f(CFP)}$ and *Ret*^{ERT2}; *Tau*$^{f(mGFP)}$ mice at E15.5, just following the time when axons of mechanosensory neurons have sent branches into layers III through V of the spinal cord (Fig. 8A–B and (Ozaki and Snider, 1997)). Mechanoreceptors typically extend a single central branch (step 1) at ~E10.5, which bifurcates upon reaching the spinal cord, projecting in both the rostral and caudal directions (step 2). Interstitial branches then form from these longitudinal projections and penetrate deep into the spinal cord (step 3) beginning ~E13.5. Then, axonal branches in the spinal cord elaborate complicated collaterals within the proper layers of the dorsal horn (step 4) beginning ~E15.5 (Fig. 8C). To visualize individual axons of control and *Ret* null RA mechanoreceptors, a low dose of 4-HT was used to label 6 ± 2 GFP^{+} neurons /DRG in control *Ret*^{ERT2}; *Tau*$^{f(mGFP)}$ mice and 11 ± 4 CFP^{+} neurons/DRG in experimental *Ret*$^{ERT2/f(CFP)}$ mice (Figure 8D–F). We found that the initial central and peripheral axonal branches of labeled fibers within the DRGs are comparable in *Ret*^{ERT2}; *Tau*$^{f(mGFP)}$ control (Figure 8D) and *Ret*$^{ERT2/f(CFP)}$ mutant mice (Figure 8E). Moreover, many labeled axons projecting rostrally and caudally in the dorsal funiculus, observed using sagittal sections of the thoracic spinal cord, were present in mice of both genotypes (Figure 8G–H). These findings indicate that axonal extension and branching steps 1 and 2 occur normally in *Ret* null RA mechanoreceptors. However, very few third-order axonal branches emanating from the longitudinal projections of *Ret* null RA mechanoreceptors were observed in *Ret*$^{ERT2/f(CFP)}$ mutant mice (0.19 ± 0.05 third-order branches/200μm rostral-caudal fiber), which is in marked contrast to the large number of these interstitial branches seen in *Ret*^{ERT2}; *Tau*$^{f(mGFP)}$ controls (1.48 ± 0.41 third-order branches/200μm rostral-caudal fiber, Figure 8G–I). This phenotype is also observed when the afferent branches are visualized using horizontal sections through the lumbar spinal cord (Figure 8J–K). Thus, Ret is required at the step 3, for the formation or extension of third-order interstitial branches of RA mechanoreceptors into the spinal cord.

Discussion

We have developed a genetic labeling strategy to show that the early-born Ret^{+} DRG neurons develop into RA mechanoreceptors, which form Meissner corpuscles, Pacinian corpuscles and longitudinal lanceolate endings. Interestingly, these RA mechanoreceptors innervate discrete target zones within the gracile and cuneate nuclei, revealing a modality-specific pattern of mechanosensory neuron axonal projections within the brainstem. In addition, we show that NRTN–GFRα2/Ret signaling is essential for development of Pacinian corpuscles and, importantly, Ret signaling mediates the formation of central connections of most if not all RA mechanosensory neurons in the spinal cord and medulla. Thus, Ret signaling orchestrates the assembly of RA mechanosensory neurons into circuits that underlie tactile discrimination and the perception of touch.

Modality-specific segregation of mechanosensory axons in the dorsal column-medial lemniscal pathway

DRG mechanoreceptors send axonal branches to local circuit neurons located in lamina III through V of the spinal cord (Brown, 1981) as well as on second order projection neurons located in the cuneate and gracile nuclei of the medulla. The DCN, in turn, convey somatosensory information to the thalamus and somatosensory cortex (Carpenter MB, 1983).

Although it is generally appreciated that topographic maps are represented within each of the projections of somatosensory pathways, from the spinal cord to the somatosensory cortex, less is known about modality maps in which RA and SA mechanosensory information is segregated. Interestingly, physiological recordings have pointed to the existence of distinct RA and SA zones along the entire extent of the dorsal-column-medial lemniscal pathway (Dykes, 1983; Dykes et al., 1982; Mountcastle, 1957; Mountcastle, 1984; Rasmusson and Northgrave, 1997). Our findings show that afferents of GFP-labeled early Ret^+ neurons almost completely fill the gracile nucleus and this nucleus is remarkably smaller in *Ret* mutant animals, suggesting that RA mechanoreceptors constitute the majority of fibers that innervate the gracile nucleus. Remarkably, the pattern of Ret^+ RA mechanosensory afferent terminations within the mouse DCN described in the present study bears striking resemblance to that found by Dykes and colleagues (Dykes et al., 1982) using physiological recordings in cats. In addition, our results provide an anatomical basis of "modality re-sorting" (Whitsel et al., 1969), a phenomenon in which RA and SA mechanosensory afferents ascending within the gracile and cuneate fasciculi of the DC reorganize such that RA mechanosensory afferents predominate in the gracile fasciculus at cervical levels. Indeed, our labeling experiments show that Ret^+ RA mechanoreceptor afferents are greatly enriched in the cervical gracile fasciculus. The observed enrichment of these RA mechanosensory afferents within the gracile fasciculus of the DC, prior to innervation of the DCN, could provide a mechanistic explanation for the formation of modality maps within the DCN. In fact, a similar mechanism of pre-target sorting of axons has been suggested for the establishment of topographic maps in the olfactory system (Imai et al., 2009). Taken together with previous physiological recordings in the cat, raccoon and monkey, our genetic labeling results from mice strongly support the existence of modality maps within the DC and DCN and the idea that such maps are found in many mammalian species.

Pacinian corpuscles require NRTN–GFRα2/Ret signaling during development but not in adulthood

We show that development of Pacinian corpuscles is dependent upon NRTN, GFRα2 and Ret. Indeed, our finding of a common phenotype in *NRTN, GFRα2 and* $Ret^{f/f};Wnt1^{Cre}$ mutant mice strongly supports the conclusion that GFRα2 is the Ret co-receptor in RA mechanoreceptors, and that a NRTN–GFRα2/Ret signaling cascade in these neurons controls Pacinian corpuscle formation. Our results further show that NRTN-GFRα2/Ret signaling is not required for maintenance of the corpuscle, once it has formed. This conclusion is based on the observation that deletion of *Ret* in three-week old mice, a time when Pacinian corpuscles are mature (Zelena, 1976), has no obvious effect on corpuscle number or morphology, even in mice up to six months of age. In contrast, Ret is required for both development (Luo et al., 2007) and maintenance (this study) of projections of at least one class of Ret^+ DRG sensory neurons, the cutaneous endings of non-peptidergic nociceptors. In all, our findings define the first growth factor signaling module required for development of Pacinian corpuscle and show that Ret is differentially required for the maintenance of axonal projections of select classes of Ret^+ DRG neurons.

Distinct roles of Ret and TrkB in the development of axonal projections of cutaneous RA mechanoreceptors

In contrast to the severe deficit of Pacinian corpuscles, the phenotypes associated with cutaneous RA mechanosensory end-organs of *Ret* mutant mice are relatively modest. Moreover, consistent with previous studies using *TrkB* null mutants (Gonzalez-Martinez et al., 2004; Perez-Pinera et al., 2008), we found that TrkB functions within cells of neural crest origin to support formation of Meissner corpuscles, pointing to a role in either the axon, Schwann cell or both. Since many early Ret^+ neurons express *TrkB* during development, we favor a model in which TrkB signaling within Ret^+ RA mechanoreceptors serves to direct the formation of Meissner corpuscles. Alternatively, since Meissner corpuscles can be innervated by either one or two Aβ fibers (Ide, 1976), and Ret and TrkB expression patterns in the DRG do not completely overlap, it is possible that some Meissner corpuscles are innervated by two molecularly distinct subtypes of Aβ fibers, each expressing either *Ret* or *TrkB*, and that the $TrkB^+$ fibers instruct the process of corpuscle formation. Either way, it is clear that Ret plays a relatively minor role in the formation of Meissner corpuscles. In striking contrast, Ret is absolutely essential for extension of interstitial branches of central axons of RA mechanoreceptors in the spinal cord whereas TrkB signaling is dispensable for the formation of these central projections. Therefore, Ret and TrkB signaling differentially support the growth and branching of central axons of RA mechanoreceptors and the formation of cutaneous RA mechanosensory end-organs.

It is also interesting to note that Ret is differentially required for development of the central projections of distinct classes of Ret^+ DRG neurons. Although dispensable for the central projections of Ret^+ non-peptidergic nociceptors (Luo et al., 2007), we show here that Ret plays a critical role in the formation of central projections of RA mechanoreceptors and hence their synaptic connections in the spinal cord and brain stem. Based on this observation, we propose that NRTN and perhaps other Ret ligands may be effective in supporting regeneration of central axonal projections of RA mechanosensory neurons, which could enable functional recovery of tactile discrimination and the perception of touch following nerve or spinal cord damage.

Method and Materials

Mouse lines and treatments

The details of Ret^{ERT2} mouse generation can be found in the supplemental materials. Ret-conditional CFP mice ($Ret^{f(CFP)}$) were generated as described (Uesaka et al., 2008). The Tau-conditional mGFP mouse line ($Tau^{f(mGFP)}$) (Hippenmeyer et al., 2005) was generously provided by Drs. Gord Fishell (NYU) and Silvia Arber (Biocenter/Friedrich Miescher Institute). The $Avil^{AP}$ mouse line (Hasegawa et al., 2007) was generously provided by Dr. Fan Wang (Duke University). The $Ret^{f/f};Wnt1^{Cre}$ mouse line was described previously (Luo et al., 2007). Descriptions of other mouse lines are found in the supplemental materials.

Ret^{ERT2} and $Tau^{f(mGFP)}$ or $Ret^{f(CFP)}$ mouse lines were mated for 2 days, and plugs were checked each day. The time when a mouse was found to have plugs is considered as E0.5. In addition, mice without obvious plugs but found pregnant 10 days following the first day of mating were also considered as E10.5. Pregnant females were gavaged with 1.0~1.5mg of 4-HT per day at the indicated times. All animal treatments were done in accordance with the regulations and policies of the Johns Hopkins Animal Care and Use Committee.

In situ hybridization and double fluorescent in situ hybridization

Digoxigenin (DIG)-labeled *cRNA* probes were used for *in situ* hybridization. *In situ* hybridization probes directed against *GFRα1, GFRα2, GFRα3, Ret, TrkA*, *TrkB*, and *TrkC* were described previously (Luo et al., 2007). Details are found in the supplemental data.

Supplementary Material

Refer to Web version on PubMed Central for supplementary material.

Acknowledgments

We thanks Drs. Silvia Arber and Gord Fishell for providing $Tau^{f(mGFP)}$ mice, Fan Wang for providing $Avil^{AP}$ mice, and Michael Caterina for the TRPV3 antibody. We thank Xinzhong Dong, Alex Kolodkin, Richard Koerber, Robin Krimm, Derek Molliver, Michael Caterina and members of the Ginty laboratory for helpful discussions and comments on the manuscript. We thank Michael Rutlin, Yin Liu, Amy Strickland, and Huiying Guo for reagents and technical support. This work was supported by NIH grants NS34814 (DDG) and AG13730 (JM). DDG is an investigator of the Howard Hughes Medical Institute.

References

Airaksinen MS, Koltzenburg M, Lewin GR, Masu Y, Helbig C, Wolf E, Brem G, Toyka KV, Thoenen H, Meyer M. Specific subtypes of cutaneous mechanoreceptors require neurotrophin-3 following peripheral target innervation. Neuron. 1996; 16:287–295. [PubMed: 8789944]

Airaksinen MS, Saarma M. The GDNF family: signalling, biological functions and therapeutic value. Nat Rev Neurosci. 2002; 3:383–394. [PubMed: 11988777]

Airaksinen MS, Titievsky A, Saarma M. GDNF family neurotrophic factor signaling: four masters, one servant? Mol Cell Neurosci. 1999; 13:313–325. [PubMed: 10356294]

Albrecht, F. L. R. a. P. J. The Senses: A Comprehensive Reference. Academic Press; San Diego: 2008. Cutaneous Mechanisms of Tactile Perception: Morphological and Chemical Organization of the Innervation to the Skin; p. 1-32.

Brown, AG. Organization in the spinal cord. Heidelberg; Springer-Verlag; Berlin: New York: 1981.

Carpenter, MB.; S., J. Human Neuroanatomy. 8th edition. Williams and Wilkins; Baltimore, MD: 1983.

Carr PA, Yamamoto T, Karmy G, Baimbridge KG, Nagy JI. Analysis of parvalbumin and calbindin D28k-immunoreactive neurons in dorsal root ganglia of rat in relation to their cytochrome oxidase and carbonic anhydrase content. Neuroscience. 1989; 33:363–371. [PubMed: 2560150]

Carroll P, Lewin GR, Koltzenburg M, Toyka KV, Thoenen H. A role for BDNF in mechanosensation. Nat Neurosci. 1998; 1:42–46. [PubMed: 10195107]

Chen AI, de Nooij JC, Jessell TM. Graded activity of transcription factor Runx3 specifies the laminar termination pattern of sensory axons in the developing spinal cord. Neuron. 2006; 49:395–408. [PubMed: 16446143]

Crowley C, Spencer SD, Nishimura MC, Chen KS, Pitts-Meek S, Armanini MP, Ling LH, McMahon SB, Shelton DL, Levinson AD, et al. Mice lacking nerve growth factor display perinatal loss of sensory and sympathetic neurons yet develop basal forebrain cholinergic neurons. Cell. 1994; 76:1001–1011. [PubMed: 8137419]

Danielian PS, Muccino D, Rowitch DH, Michael SK, McMahon AP. Modification of gene activity in mouse embryos in utero by a tamoxifen-inducible form of Cre recombinase. Curr Biol. 1998; 8:1323–1326. [PubMed: 9843687]

Durbec P, Marcos-Gutierrez CV, Kilkenny C, Grigoriou M, Wartiowaara K, Suvanto P, Smith D, Ponder B, Costantini F, Saarma M. GDNF signalling through the Ret receptor tyrosine kinase. Nature. 1996; 381:789–793. [PubMed: 8657282]

Dykes RW. Parallel processing of somatosensory information: a theory. Brain Res. 1983; 287:47–115. [PubMed: 6311356]

Dykes RW, Rasmusson DD, Sretavan D, Rehman NB. Submodality segregation and receptive-field sequences in cuneate, gracile, and external cuneate nuclei of the cat. J Neurophysiol. 1982; 47:389–416. [PubMed: 6461730]

Feil R, Wagner J, Metzger D, Chambon P. Regulation of Cre recombinase activity by mutated estrogen receptor ligand-binding domains. Biochem Biophys Res Commun. 1997; 237:752–757. [PubMed: 9299439]

Fundin BT, Silos-Santiago I, Ernfors P, Fagan AM, Aldskogius H, DeChiara TM, Phillips HS, Barbacid M, Yancopoulos GD, Rice FL. Differential dependency of cutaneous mechanoreceptors on neurotrophins, trk receptors, and P75 LNGFR. Dev Biol. 1997; 190:94–116. [PubMed: 9331334]

Gonzalez-Martinez T, Farinas I, Del Valle ME, Feito J, Germana G, Cobo J, Vega JA. BDNF, but not NT-4, is necessary for normal development of Meissner corpuscles. Neurosci Lett. 2005; 377:12–15. [PubMed: 15722178]

Gonzalez-Martinez T, Germana GP, Monjil DF, Silos-Santiago I, de Carlos F, Germana G, Cobo J, Vega JA. Absence of Meissner corpuscles in the digital pads of mice lacking functional TrkB. Brain Res. 2004; 1002:120–128. [PubMed: 14988041]

Hasegawa H, Abbott S, Han BX, Qi Y, Wang F. Analyzing somatosensory axon projections with the sensory neuron-specific Advillin gene. J Neurosci. 2007; 27:14404–14414. [PubMed: 18160648]

Heuckeroth RO, Enomoto H, Grider JR, Golden JP, Hanke JA, Jackman A, Molliver DC, Bardgett ME, Snider WD, Johnson EM Jr. Milbrandt J. Gene targeting reveals a critical role for neurturin in the development and maintenance of enteric, sensory, and parasympathetic neurons. Neuron. 1999; 22:253–263. [PubMed: 10069332]

Hippenmeyer S, Vrieseling E, Sigrist M, Portmann T, Laengle C, Ladle DR, Arber S. A developmental switch in the response of DRG neurons to ETS transcription factor signaling. PLoS Biol. 2005; 3:e159. [PubMed: 15836427]

Hokfelt T. Neuropeptides in perspective: the last ten years. Neuron. 1991; 7:867–879. [PubMed: 1684901]

Hughes DI, Polgar E, Shehab SA, Todd AJ. Peripheral axotomy induces depletion of the vesicular glutamate transporter VGLUT1 in central terminals of myelinated afferent fibres in the rat spinal cord. Brain Res. 2004; 1017:69–76. [PubMed: 15261101]

Hughes DI, Scott DT, Riddell JS, Todd AJ. Upregulation of substance P in low-threshold myelinated afferents is not required for tactile allodynia in the chronic constriction injury and spinal nerve ligation models. J Neurosci. 2007; 27:2035–2044. [PubMed: 17314299]

Ide C. The fine structure of the digital corpuscle of the mouse toe pad, with special reference to nerve fibers. Am J Anat. 1976; 147:329–355. [PubMed: 983972]

Iggo A, Andres KH. Morphology of cutaneous receptors. Annu Rev Neurosci. 1982; 5:1–31. [PubMed: 6280572]

Iggo A, Muir AR. The structure and function of a slowly adapting touch corpuscle in hairy skin. J Physiol. 1969; 200:763–796. [PubMed: 4974746]

Iggo A, Ogawa H. Correlative physiological and morphological studies of rapidly adapting mechanoreceptors in cat's glabrous skin. J Physiol. 1977; 266:275–296. [PubMed: 853451]

Imai T, Yamazaki T, Kobayakawa R, Kobayakawa K, Abe T, Suzuki M, Sakano H. Pre-target axon sorting establishes the neural map topography. Science. 2009; 325:585–590. [PubMed: 19589963]

Jing S, Yu Y, Fang M, Hu Z, Holst PL, Boone T, Delaney J, Schultz H, Zhou R, Fox GM. GFRalpha-2 and GFRalpha-3 are two new receptors for ligands of the GDNF family. J Biol Chem. 1997; 272:33111–33117. [PubMed: 9407096]

Johansson RS, Vallbo AB. Tactile sensibility in the human hand: relative and absolute densities of four types of mechanoreceptive units in glabrous skin. J Physiol. 1979; 286:283–300. [PubMed: 439026]

Klein R, Silos-Santiago I, Smeyne RJ, Lira SA, Brambilla R, Bryant S, Zhang L, Snider WD, Barbacid M. Disruption of the neurotrophin-3 receptor gene trkC eliminates la muscle afferents and results in abnormal movements. Nature. 1994; 368:249–251. [PubMed: 8145824]

Kramer I, Sigrist M, de Nooij JC, Taniuchi I, Jessell TM, Arber S. A role for Runx transcription factor signaling in dorsal root ganglion sensory neuron diversification. Neuron. 2006; 49:379–393. [PubMed: 16446142]

Lawson, SN. Morphological and biochemical cell types of sensory neurons. Oxford Univeristy Press; Oxford: 1992.

Lawson SN, Caddy KW, Biscoe TJ. Development of rat dorsal root ganglion neurones. Studies of cell birthdays and changes in mean cell diameter. Cell Tissue Res. 1974; 153:399–413. [PubMed: 4458950]

Lawson SN, Perry MJ, Prabhakar E, McCarthy PW. Primary sensory neurones: neurofilament, neuropeptides, and conduction velocity. Brain Res Bull. 1993; 30:239–243. [PubMed: 7681350]

LeMaster AM, Krimm RF, Davis BM, Noel T, Forbes ME, Johnson JE, Albers KM. Overexpression of brain-derived neurotrophic factor enhances sensory innervation and selectively increases neuron number. J Neurosci. 1999; 19:5919–5931. [PubMed: 10407031]

Lindahl M, Timmusk T, Rossi J, Saarma M, Airaksinen MS. Expression and alternative splicing of mouse Gfra4 suggest roles in endocrine cell development. Mol Cell Neurosci. 2000; 15:522–533. [PubMed: 10860579]

Liu Q, Vrontou S, Rice FL, Zylka MJ, Dong X, Anderson DJ. Molecular genetic visualization of a rare subset of unmyelinated sensory neurons that may detect gentle touch. Nat Neurosci. 2007; 10:946–948. [PubMed: 17618277]

Luo W, Wickramasinghe SR, Savitt JM, Griffin JW, Dawson TM, Ginty DD. A hierarchical NGF signaling cascade controls Ret-dependent and Ret-independent events during development of nonpeptidergic DRG neurons. Neuron. 2007; 54:739–754. [PubMed: 17553423]

Marmigere F, Ernfors P. Specification and connectivity of neuronal subtypes in the sensory lineage. Nat Rev Neurosci. 2007; 8:114–127. [PubMed: 17237804]

McDonagh SC, Lee J, Izzo A, Brubaker PL. Role of glial cell-line derived neurotropic factor family receptor alpha2 in the actions of the glucagon-like peptides on the murine intestine. Am J Physiol Gastrointest Liver Physiol. 2007; 293:G461–468. [PubMed: 17585017]

Molliver DC, Wright DE, Leitner ML, Parsadanian AS, Doster K, Wen D, Yan Q, Snider WD. IB4-binding DRG neurons switch from NGF to GDNF dependence in early postnatal life. Neuron. 1997; 19:849–861. [PubMed: 9354331]

Mountcastle VB. Modality and topographic properties of single neurons of cat's somatic sensory cortex. J Neurophysiol. 1957; 20:408–434. [PubMed: 13439410]

Mountcastle, VB. Central nervous mechanisms in mechanoreceptive sensibility. In: Darian-Smith, I., editor. Handbook of Physiology. Bethesda: 1984. p. 789-879.

Oliveira AL, Hydling F, Olsson E, Shi T, Edwards RH, Fujiyama F, Kaneko T, Hokfelt T, Cullheim S, Meister B. Cellular localization of three vesicular glutamate transporter mRNAs and proteins in rat spinal cord and dorsal root ganglia. Synapse. 2003; 50:117–129. [PubMed: 12923814]

Ozaki S, Snider WD. Initial trajectories of sensory axons toward laminar targets in the developing mouse spinal cord. J Comp Neurol. 1997; 380:215–229. [PubMed: 9100133]

Pare M, Smith AM, Rice FL. Distribution and terminal arborizations of cutaneous mechanoreceptors in the glabrous finger pads of the monkey. J Comp Neurol. 2002; 445:347–359. [PubMed: 11920712]

Patel TD, Jackman A, Rice FL, Kucera J, Snider WD. Development of sensory neurons in the absence of NGF/TrkA signaling in vivo. Neuron. 2000; 25:345–357. [PubMed: 10719890]

Perez-Pinera P, Garcia-Suarez O, Germana A, Diaz-Esnal B, de Carlos F, Silos-Santiago I, del Valle ME, Cobo J, Vega JA. Characterization of sensory deficits in TrkB knockout mice. Neurosci Lett. 2008; 433:43–47. [PubMed: 18248898]

Rasmusson DD, Northgrave SA. Reorganization of the raccoon cuneate nucleus after peripheral denervation. J Neurophysiol. 1997; 78:2924–2936. [PubMed: 9405513]

Smeyne RJ, Klein R, Schnapp A, Long LK, Bryant S, Lewin A, Lira SA, Barbacid M. Severe sensory and sympathetic neuropathies in mice carrying a disrupted Trk/NGF receptor gene. Nature. 1994; 368:246–249. [PubMed: 8145823]

Trupp M, Arenas E, Fainzilber M, Nilsson AS, Sieber BA, Grigoriou M, Kilkenny C, Salazar-Grueso E, Pachnis V, Arumae U. Functional receptor for GDNF encoded by the c-ret proto-oncogene. Nature. 1996; 381:785–789. [PubMed: 8657281]

Uesaka T, Nagashimada M, Yonemura S, Enomoto H. Diminished Ret expression compromises neuronal survival in the colon and causes intestinal aganglionosis in mice. J Clin Invest. 2008; 118:1890–1898. [PubMed: 18414682]

Whitsel BL, Petrucelli LM, Sapiro G. Modality representation in the lumbar and cervical fasciculus gracilis of squirrel monkeys. Brain Res. 1969; 15:67–78. [PubMed: 4241233]

Zelena J. The role of sensory innervation in the development of mechanoreceptors. Prog Brain Res. 1976; 43:59–64. [PubMed: 130653]

Zelena, J. Nerves and Mechanoreceptors. Chapman & Hall; London: 1994.

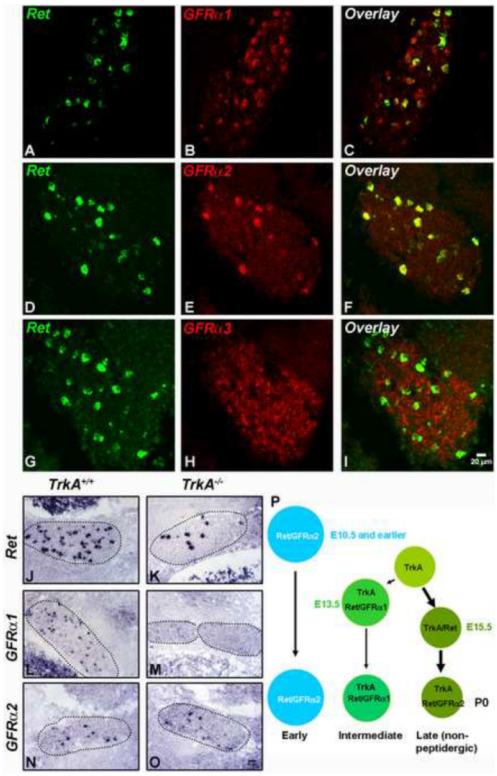

Figure 1. The early Ret$^+$ DRG neurons express *GFRα2*

Double fluorescent *in situ* hybridization of *Ret* and *GFRα1* (A–C), *Ret* and *GFRα2* (D–F), and *Ret* and *GFRα3* (G–I) at E13.5 (n=3, and 6 to 8 sections were examined for each animal, lower lumbar DRGs). J–O: *In situ* hybridization of *Ret* (37 ± 6 vs. 7 ± 3), *GFRα1* (29 ± 3 vs. 0), and *GFRα2* (10 ± 3 vs. 9 ± 1) in control and *TrkA* null DRGs at E13.5 (control vs. mutant, mean ± SEM positive neurons/section, n=3 animals per genotype, and 6 to 8 sections were examined and quantified for each animal, lower lumbar DRGs). P. Illustration of the three populations of Ret$^+$ DRG neurons based on their developmental origin and temporal patterns of expression of *Ret* and *GFRα* co-receptors.

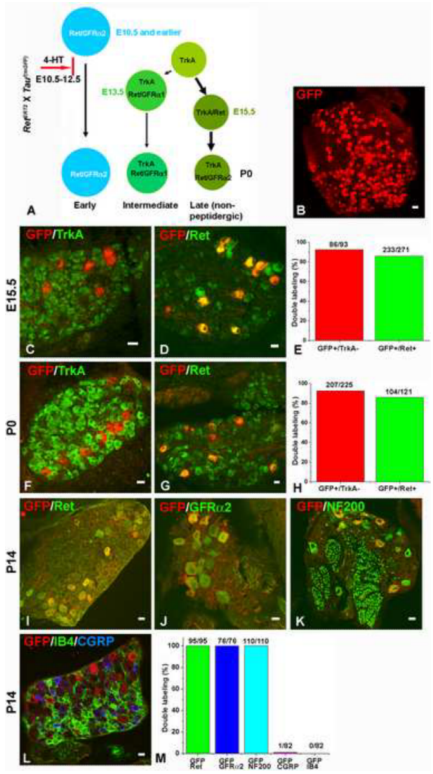

Figure 2. Genetic Labeling of the early Ret$^+$ DRG neurons

A. Outline of the chemical-genetic strategy for labeling the early Ret$^+$ neurons. *Ret^{ERT2}* and *Tau$^{f(mGFP)}$* mice were crossed, and timed pregnant mothers were gavaged with 1.0 to 1.5 mg 4-HT per day from E10.5 to E12.5. B. Whole-mount anti-GFP immunostaining of a labeled L5 DRG. 280 ± 25 GFP$^+$ neurons were labeled. Eight L5 DRGs from four animals of two litters were examined. C–D: Double immunostaining of GFP with TrkA (C) or Ret (D) in E15.5 labeled DRGs. 86/93 (GFP$^+$/TrkA$^-$ neurons / total GFP$^+$ neurons) GFP$^+$ neurons are TrkA$^-$, and 233/271 (GFP$^+$/Ret$^+$ neurons / total GFP$^+$ neurons) GFP$^+$ neurons are Ret$^+$. Lumbar DRGs, n=6 from three litters. 4–6 sections from each animal were quantified and shown in E. F–G: Double immunostaining of GFP with TrkA (F) or Ret (G) in P0 labeled DRGs. 207/225 (92%) GFP$^+$ neurons are TrkA$^-$, and 104/121 (86%) GFP$^+$ neurons are Ret$^+$. Lumbar DRGs, n=7 from four litters for GFP/TrkA staining, and n=4 from two litters for GFP/Ret staining. Quantifications are shown in H. I–L: Double immunostaining of GFP and Ret (I), GFP and GFRα2 (J), GFP and NF200 (K), and GFP and CGRP and IB4 in P14 labeled DRGs. All GFP$^+$ neurons (95/95) are Ret$^+$ at this time (Note that, due to the fixation conditions needed for this experiment, Ret immunoreactivity is detected only in those DRG neurons expressing a high level of Ret protein). In addition, GFP$^+$ neurons are GFRα2$^+$ (76/76) and NF200$^+$ (110/110), but not CGRP$^+$ (1/82) or IB4$^+$ (0/82). Quantifications are shown in M. Lumbar DRGs, n=4 from two litters. Scale bar for panel B: 50μm, other panels: 20μm

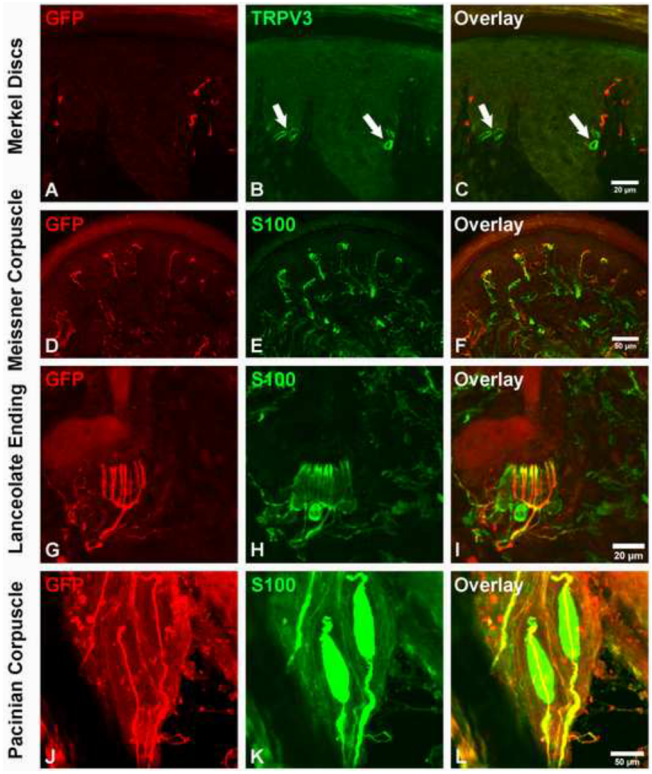

Figure 3. The early Ret$^+$ DRG neurons are the RA mechanoreceptors associated with Meissner corpuscles, Pacinian corpuscles and longitudinal lanceolate endings

A–C: GFP$^+$ fibers do not innervate Merkel cells in the footpad (339/356 {95.2%} of Merkel cells, labeled with the TrpV3 antibody, are not associated with GFP$^+$ axons). The locations of Merkel cells are indicated by white arrows. D–F: GFP$^+$ fibers innervate Meissner corpuscles, visualized by S100 immunostaining, in dermal papillae (114/172 {66.3%} Meissner corpuscles are innervated by GFP$^+$ fibers). G–I: GFP$^+$ fibers form longitudinal lanceolate endings associated with hair follicles, shown by S100 immunostaining (78/184 {42.3%} of hair follicles are associated with GFP$^+$ longitudinal lanceolate endings). J–L: Whole-mount anti-GFP and anti-S100 staining of the periosteum membrane of the fibula. Note that a single GFP$^+$ fiber innervates each Pacinian corpuscle (55/60 {91.7%} of Pacinian corpuscles are innervated by GFP$^+$ fibers). Immunostainings were performed using P14 $Ret^{ERT2};Tau^{f(mGFP)}$ mice treated with 4-HT from E10.5 and E12.5. Quantifications were made using four P14 $Ret^{ERT2};Tau^{f(mGFP)}$ mice from two litters.

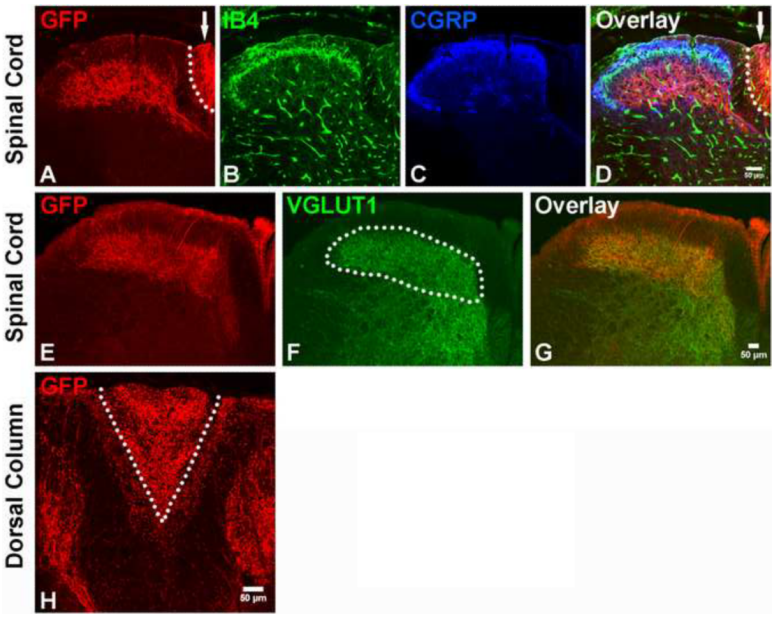

Figure 4. Central projections of early Ret$^+$ DRG neurons innervate layers III through V of the spinal cord

A–D: Central projections of GFP labeled early Ret$^+$ DRG neurons in the upper lumbar level of the spinal cord. Note the presence of GFP$^+$ fibers in both lamina III through V of the spinal cord and the dorsal column (arrow indicates the area which is also outlined by the dotted line). Nociceptor axons innervating spinal cord layers I and II were visualized with CGRP immunostaining (blue) and IB4 binding (green), respectively. E–G: Double staining of GFP and VGLUT1. VGLUT1 labels synapses of the central projections of mechanoreceptors (white dotted line) and proprioceptors (Hughes et al., 2004; Oliveira et al., 2003). H: Dorsal column of the cervical spinal cord. Note that while GFP$^+$ fibers are present in both the gracile (V shape tract, inside the white dotted line) and cuneate fasiculi (area outside the white dotted line), they are greatly enriched in the gracile fasiculus. N=4 from two litters for P14 *Ret^{ERT2};Tau$^{f(mGFP)}$* mice treated with 4-HT from E10.5 to E12.5.

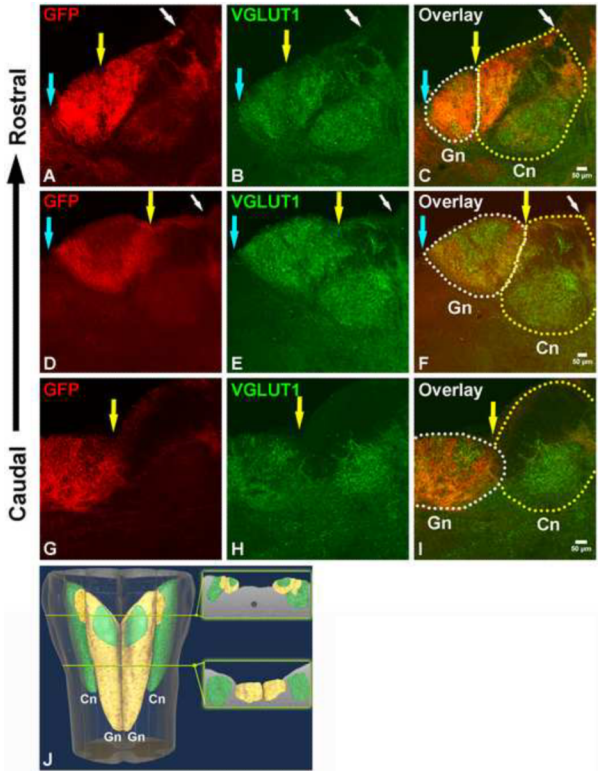

Figure 5. Modality-specific segregation of mechanosensory axons in dorsal column nuclei

A, D, G: GFP$^+$ fibers innervating the gracile and cuneate nuclei at different rostral to caudal levels of the medulla. The VGLUT1 staining is used to visualize the gracile and cuneate nuclei (B, E, H). The white dotted line outlines the boundary of the gracile nucleus (Gn), and the yellow dotted line outlines the boundary of the cuneate fasiculus and nucleus (Cn) in C, F, I. Note that GFP$^+$ fibers occupy most of the gracile nucleus (I), but are absent from a dorsal segment at the mid-level of the medulla (F). On the other hand, GFP$^+$ fibers do not innervate the caudal-ventral region of the cuneate nucleus (F and I), but project to the dorsal-rostral region of the cuneate nucleus (C). Arrows indicate the boundaries of the gracile and cuneate nuclei. J. Three-dimensional illustration of the pattern of innervation of the gracile and cuneate nuclei by RA mechanoreceptors. This model is based upon the findings reported in Fig. 5A–I and fig S7. The VGLUT1$^+$ zones occupied by GFP$^+$ fibers are showed in yellow. The green zones are unoccupied VGLUT1$^+$ zones. N=3 for 2 month old *Ret*^{ERT2};*Tau*$^{f(mGFP)}$ mice treated with 4-HT from E10.5 to E12.5.

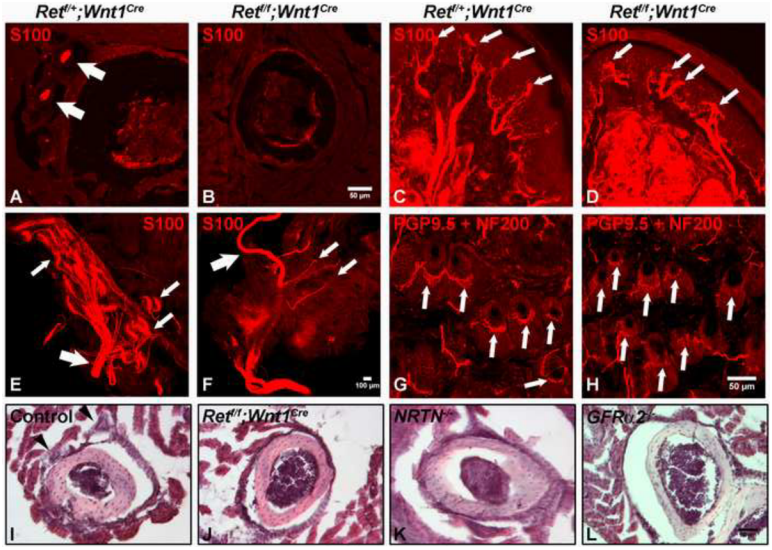

Figure 6. NRTN-GFRα2/Ret signaling is required for development but not maintenance of Pacinian corpuscles

A–B: Anti-S100 immunostaining of Pacinian corpuscles (white arrows) in the periosteum of the fibula of P14 control and $Ret^{f/f};Wnt1^{Cre}$ mice. Pacinian corpuscles (white arrows) are completely absent (35 ± 5 control vs. 0 mutant, per side) in the $Ret^{f/f};Wnt1^{Cre}$ mice, as visualized using both sections and whole-mount staining (E–F). C–D: Staining of Meissner corpuscles in P14 control and $Ret^{f/f};Wnt1^{Cre}$ mice. Meissner corpuscles (white arrows) appear in normal number in the absence of Ret signaling. However, the morphology of Meissner corpuscles in $Ret^{f/f};Wnt1^{Cre}$ mice is slightly disorganized relative to those found in control mice. E–F: Anti-S100 whole mount immunostaining of Pacinian corpuscles from P14 control and $Ret^{f/f};Wnt1^{Cre}$ mice, Large arrows indicate the interosseous nerve. In the control periosteum membrane, sensory nerves exhibit a tree-like structure on which Pacinian corpuscles are formed (small white arrows indicate a few examples). In contrast, only a few small nerve branches are present (small white arrows), but neither Pacinian corpuscles nor the tree-like nerve branch structures are observed in the $Ret^{f/f};Wnt1^{Cre}$ periosteum membrane, suggesting RA mechanosensory nerves are not present in the absence of *Ret*. G–H: Staining of longitudinal lanceolate endings (white arrows) in P14 control and $Ret^{f/f};Wnt1^{Cre}$ mice. Longitudinal lanceolate endings are present in $Ret^{f/f};Wnt1^{Cre}$ mice, although they appear morphologically underdeveloped. Higher magnification and quantification of these endings are shown in fig. S11A–C. I–L: H & E staining of Pacinian corpuscles in P14 control (black arrow heads), $Ret^{f/f};Wnt1^{Cre}$, *NRTN* null and $GFR\alpha2^{GFP}$ null mice. H & E staining is used here to rule out the potential confounding issue of decreased S100 expression in mutant mice. N≥3 for each mutant genotype.

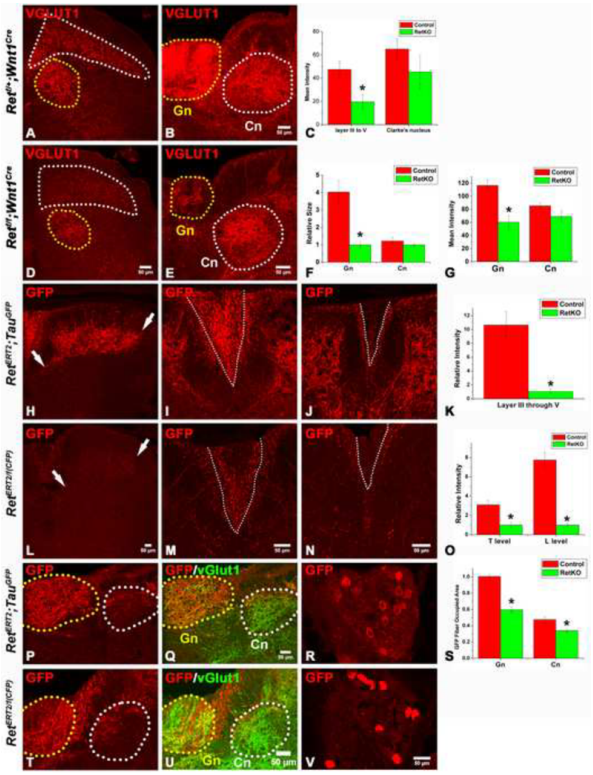

Figure 7. RA mechanoreceptors require Ret signaling for their assembly into mechanosensory circuits in the spinal cord and medulla

A–B: Synapses of mechanoreceptors, visualized by VGLUT1 staining, in the upper lumbar spinal cord and mid-level medulla of P14 control mice. D–E: Synapses of mechanoreceptors in the upper lumbar spinal cord and mid-level medulla of P14 $Ret^{f/f}; Wnt1^{Cre}$ mice. Layers III through V of the spinal cord are outlined by the white dotted line, and Clarke's nucleus is outlined by the yellow dotted line. In the medulla, the gracile nucleus is outlined by the yellow dotted line, and the cuneate nucleus is outlined by the white dotted line. The VGLUT1 staining intensity in layer III through V of spinal cord and gracile nucleus of mutant mice is much lower than that of controls. Quantification of spinal cord staining intensity is shown in panel C (Student's *t* test, P<0.001 for layers III through V), quantification of the size of the gracile and cuneate nuclei is shown in F (Student's *t* test, P<0.001 for the gracile nucleus), and quantification of the intensity of the medulla staining is shown in G (Student's *t* test, P<0.001 for the gracile nucleus). H,L: Anti-GFP staining of RA mechanoreceptor central axonal projections into the spinal cord of P14 $Ret^{ERT2};Tau^{f(mGFP)}$ (control) and $Ret^{ERT/f(CFP)}$ (Ret KO) mice, which were treated with 4-HT at E11.5 and E12.5. Note the reduction in the number of GFP^+ axons in $Ret^{ERT/f(CFP)}$ mice. White arrows indicate the range of projections. Quantification of relative intensity of GFP^+ fibers is shown in K. The difference between control and *Ret* null neurons is statistically significant (Student's *t* test, P<0.001). I, J: Anti-GFP staining of the dorsal columns of P14 $Ret^{ERT2};Tau^{f(mGFP)}$ mice at thoracic (I) and lumbar (J) levels. M,N: Anti-GFP staining of the dorsal columns of P14 $Ret^{ERT/f(CFP)}$ mice at thoracic (M) and lumbar (N) levels. Many fewer CFP^+ fibers are found in the gracile fasciculus of the dorsal column of the mutant (outlined by white dotted lines). Quantification is shown in O. The difference between the control and *Ret* null neurons is statistically significant (Student's *t* test, P< 0.001 for the lumbar level, and P<0.01 for the thoracic level). P,Q: Anti-GFP staining of RA mechanosensory fibers innervating the medulla in P14 $Ret^{ERT2};Tau^{f(mGFP)}$ mice. T–U: Anti-GFP staining of RA mechanosensory innervation of the medulla in P14 $Ret^{ERT/f(CFP)}$

mice. The relative area occupied by GFP^+ fibers within the gracile (Gn) and cuneat nucleus (Cn) is quantified in S. The difference between the control and *Ret* null neurons is statistically significant (Student's *t* test, $P<0.01$ for the gracile nucleus, and $P<0.05$ for the cuneate nucleus). R, V: GFP labeled RA mechanosensory DRG neurons in $Ret^{ERT2};Tau^{f(mGFP)}$ and $Ret^{ERT/f(CFP)}$ thoracic DRGs at P14. On average, 8 ± 3 neurons/section are labeled by GFP in $Ret^{ERT2};Tau^{f(mGFP)}$ mice while 6 ± 2 neurons/section are labeled by CFP in $Ret^{ERT/f(CFP)}$ mice. Note that the level of expression of CFP in *Ret* null neurons is higher than that of control neurons. N=3 for control and $Ret^{f/f};Wnt1^{Cre}$ mice and N=3 for both $Ret^{ERT2};Tau^{f(mGFP)}$ and $Ret^{ERT/f(CFP)}$ mice. 8 to 12 spinal cord sections per animal for each genotype were examined and quantified.

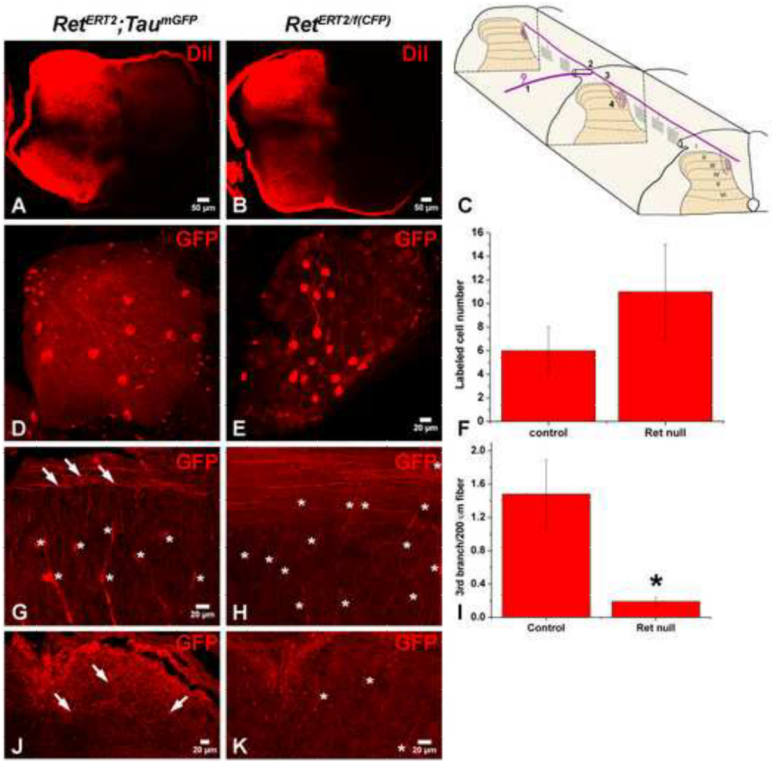

Figure 8. Ret is required autonomously for the formation of the 3rd branch of central RA mechanosensory axons

A–B: DiI labeling of thoracic DRGs of E15.5 *Ret*^{ERT2};*Tau*$^{f(mGFP)}$ and *Ret*$^{ERT/f(CFP)}$ mice. Consistent with published findings (Ozaki and Snider, 1997), mechanoreceptors have already extended central axonal projections to spinal cord layers III through V at E15.5. C: Illustration of RA mechanoreceptor central projections, which can be subdivided into four steps. This illustration is adapted from (Brown, 1981). D: Whole mount anti-GFP staining of a control *Ret*^{ERT2};*Tau*$^{f(mGFP)}$ DRG from an animal treated with 0.6mg of 4-HT. Note that the 1st order central projections are visible in the DRG. On average, 6 ± 2 GFP$^+$ neurons are labeled per thoracic DRG (12 DRGs in total, N=3 from two separate litters). E: Whole mount anti-GFP staining of a *Ret*$^{ERT/f(CFP)}$ DRG from an animal treated with 1mg of 4-HT. Note that 1st order central projections are visible in the DRG. On average, 11 ± 4 CFP$^+$ neurons are labeled per thoracic DRG (20 DRGs in total, N=4 from three separate litters). F: Quantification of labeled DRG neuron number. G: Anti-GFP staining with sagittal thoracic spinal cord sections of *Ret*^{ERT2};*Tau*$^{f(mGFP)}$ mice. Note that the 3rd order axonal branches (white arrows) originate from rostral-caudal running fibers and penetrate the spinal cord. "*" indicates the position of blood vessels which are autofluorescent and seen in mice of both genotypes. H: Anti-GFP staining of sagittal thoracic spinal cord sections of *Ret*$^{ERT/f(CFP)}$ mice. Note that very few 3rd order axonal branches originating from rostral-caudal running fibers are found in these mice. I: Quantification of the numer of 3rd order axonal branches for the two genotypes. On average, 1.48 ± 0.41 3rd order axonal branches are observed in every 200μm rostral-caudal fiber in *Ret*^{ERT2};*Tau*$^{f(mGFP)}$ control mice (N=3 from two litters, and more than 100 rostralcaudal fibers were measured) while 0.19 ± 0.05 3rd order axonal branches are observed in every 200μm rostral-caudal fiber in *Ret*$^{ERT/f(CFP)}$ mutant mice (N=4 from three litters, and more than 100 rostral-caudal fibers were measured). J–K: Anti-GFP staining using horizontal lumbar spinal cord sections taken from *Ret*^{ERT2};*Tau*$^{f(mGFP)}$ (J) and *Ret*$^{ERT/f(CFP)}$ (K) mice. Similar to that observed using sagittal thoracic sections,

there are several GFP$^+$ central projections in *Ret*^{ERT2};*Tau*$^{f(mGFP)}$ control mice at this age, but almost no CFP$^+$ central projections are found in the *Ret*$^{ERT/f(CFP)}$ mice.